

Journal of Visualized Experiments

High Sensitivity Measurement of Transcription Factor-DNA Binding Affinities by Competitive Titration Using Fluorescence Microscopy

--Manuscript Draft--

Article Type:	Invited Methods Article - JoVE Produced Video
Manuscript Number:	JoVE58763R3
Full Title:	High Sensitivity Measurement of Transcription Factor-DNA Binding Affinities by Competitive Titration Using Fluorescence Microscopy
Keywords:	Transcription factor, protein-DNA interaction, binding specificity, binding affinity, fluorescence anisotropy, segmentation network.
Corresponding Author:	Christophe Jung GERMANY
Corresponding Author's Institution:	
Corresponding Author E-Mail:	jung@genzentrum.lmu.de
Order of Authors:	Christophe Jung Max Schnepf Peter Bandilla Ulrich Unnerstall Ulrike Gaul
Additional Information:	
Question	Response
Please indicate whether this article will be Standard Access or Open Access.	Open Access (US\$4,200)
Please indicate the city, state/province, and country where this article will be filmed . Please do not use abbreviations.	Munich, Bavaria, Germany

TITLE:

High Sensitivity Measurement of Transcription Factor-DNA Binding Affinities by Competitive Titration Using Fluorescence Microscopy

AUTHORS AND AFFILIATIONS:

Christophe Jung¹, Max Schnepf¹, Peter Bandilla¹, Ulrich Unnerstall¹, Ulrike Gaul¹

¹Gene Center and Department of Biochemistry, Center for Protein Science Munich (CIPSM), Ludwig-Maximilians-Universität München, Feodor-Lynen-Strasse, München, Germany

Corresponding Author:

Christophe Jung (jung@genzentrum.lmu.de)

Email Addresses of Co-Authors:

Max Schnepf (schnepf@genzentrum.lmu.de)

Peter Bandilla (bandilla@genzentrum.lmu.de)

Ulrich Unnerstall (unnerstall@genzentrum.lmu.de)

Ulrike Gaul (gaul@genzentrum.lmu.de)

KEYWORDS:

Transcription factor, protein-DNA interaction, binding specificity, binding affinity, fluorescence anisotropy, segmentation network

SUMMARY:

Here we present a novel method for determining binding affinities at equilibrium and in solution with high sensitivity on a large scale. This improves the quantitative analysis of transcription factor-DNA binding. The method is based on automated fluorescence anisotropy measurements in a controlled delivery system.

ABSTRACT:

Accurate quantification of transcription factor (TF)-DNA interactions is essential for understanding the regulation of gene expression. Since existing approaches suffer from significant limitations, we have developed a new method for determining TF-DNA binding affinities with high sensitivity on a large scale. The assay relies on the established fluorescence anisotropy (FA) principle but introduces important technical improvements. First, we measure a full FA competitive titration curve in a single well by incorporating TF and a fluorescently labeled reference DNA in a porous agarose gel matrix. Unlabeled DNA oligomer is loaded on the top as a competitor and, through diffusion, forms a spatio-temporal gradient. The resulting FA gradient is then read out using a customized epifluorescence microscope setup. This improved setup greatly increases the sensitivity of FA signal detection, allowing both weak and strong binding to be reliably quantified, even for molecules of similar molecular weights. In this fashion, we can measure one titration curve per well of a multi-well plate, and through a fitting procedure, we can extract both the absolute dissociation constant (K_D) and active protein concentration. By testing all single-point mutation variants of a given consensus binding sequence, we can survey

the entire binding specificity landscape of a TF, typically on a single plate. The resulting position weight matrices (PWMs) outperform those derived from other methods in predicting *in vivo* TF occupancy. Here, we present a detailed guide for implementing HiP-FA on a conventional automated fluorescent microscope and the data analysis pipeline.

INTRODUCTION:

Given the central role of transcription factors (TFs) in gene regulation, determining their binding preferences in a quantitative manner is of paramount importance. Seminal studies by von Hippel introduced the notion that regulatory TFs rapidly recognize DNA, such that their binding is well described by the thermodynamic equilibrium, while the downstream events of recruiting RNA polymerase to the promoter are controlled by slower kinetics¹. Recent *in vivo* binding studies suggest that this picture is likely more complex^{2,3}; nevertheless, these general assumptions serve as good approximations and have supported many computational approaches to find cis-regulatory elements and predict expression from sequences⁴⁻⁶. While equilibrium binding has thus been successfully employed as a concept, current methods for determining TF-DNA interactions focus on binding specificity and typically do not directly measure binding affinities at equilibrium. The systematic measurement of TF-DNA binding represents a considerable technical challenge, and the existing methods have several different limitations.

Chromatin immunoprecipitation followed by deep sequencing (ChIP-seq)⁷, the most prevalent *in vivo* technique, does not permit the measurement of binding affinities or the precise localization of binding sites within genomic fragments. Several *in vitro* methods, including DNase footprinting⁸, electrophoretic mobility shift (EMSA)⁹, surface plasmon resonance (SPR)¹⁰, and microscale thermophoresis¹¹ are able to measure binding affinities, but they are relatively low throughput. Conversely, high throughput techniques including protein binding microarrays¹², HT-SELEX^{13,14}, and bacterial one-hybrid (B1H)¹⁵ are not able to measure binding affinities and typically yield overly specific binding sequences, which is mainly due to the stringent selection or washing steps necessary. More recent developments include the deep sequencing based HiTS-FLIP¹⁶, SELEX-seq¹⁷, and the microfluidics-based MITOMI¹⁸ or SMILE-Seq¹⁹, which allow for extraction of absolute binding affinities; however, they rely on measuring fluorescence intensities of labeled TF and DNA. Fluorescence signals, therefore, become limiting at low protein concentrations and in determining low K_D values ($< \sim 10$ nM). Moreover, the TF-DNA binding in these methods takes place on thin surfaces, raising issues with unspecific binding and/or auto-fluorescence background, which makes it difficult to accurately quantify weak binding.

To address these limitations, we have developed a new method to determine TF-DNA affinity landscapes at equilibrium and in solution, which we called high performance fluorescence anisotropy (HiP-FA)²⁰. The technique is based on the established fluorescence anisotropy (FA) assay²¹ but modified to measure binding constants with high sensitivity and at large-scale using a customized automated microscope and analysis setup.

The FA assay monitors the interaction of fluorescently labeled species (like a DNA oligomer) to a binding partner, in this case a TF, by measuring the molecular rotation of the labeled molecule. Upon binding to the TF, its rotational speed decreases due to the higher hydrodynamic radius

and molecular weight of the bound complex, which results in increased FA. The accurate measurement of very strong binding ($K_D < \sim 1$ nM) requires the use of low concentrations of labeled, reference DNA ($c < \sim 1$ nM). This is difficult to achieve with a commercial instrument such as a standard microplate reader. In addition, a large size difference (10-100 fold) between the bound and unbound complexes is usually necessary, prohibiting measurement of interactions between TF binding domains and short DNA oligomers, which are typically of roughly similar molecular weights. Finally, a full titration curve normally requires the preparation and measurement of multiple wells containing a concentration series for the titrating species.

To address these issues, we use a widefield microscopy setup, modified to achieve high detection sensitivity and allow FA measurements at different z-positions of a single well. This enables us to monitor binding interactions between species of similar molecular weight and with high affinities. Higher throughput is achieved by measuring FA in multi-well plate formats and carrying out an entire titration series in a single well using a controlled delivery system (**Figure 1a**). Furthermore, by employing a competitive binding assay, we extract not only the binding constants but also the concentration of active protein. This is an important feature of the assay, since only a portion of the expressed TF molecules are active due to protein misfolding or degradation. The experimental setup is based on a commercial epifluorescence microscope equipped with XY- and Z- piezo stages. We upgraded the system with external laser excitation, then detected the two emitted linear polarization components on the chip of an EM-CCD camera with high quantum efficiency for light detection (**Figure 1b** and **1c**). The system uses a high numerical aperture (NA) objective coupled to an ultra-sensitive sensor and thus affords highly sensitive FA measurements. By recording fluorescence z-stacks, binding interactions can be measured along the optical z-axis when using a heterogeneous matrix for the reactants. All these modifications can be readily implemented on an existing system and are cost-effective.

We employ a competitive binding assay in which the binding affinity of an unlabeled DNA oligomer is measured in comparison to the fluorescently labeled DNA, which serves as a reference. TF and reference DNA are incorporated at fixed concentrations in a porous agarose gel matrix (pore size ~ 1 μ m) that constitutes a non-interacting environment for the binding. The reference DNA is labeled with Cy5. This dye proved to be well-suited for FA measurements due to its relatively long fluorescence lifetime (~ 1 ns) and fluorescence emission in the far-red of the visible spectrum (low auto-fluorescence background). The TF concentration is in molar excess over Cy5-reference DNA, ensuring that all reference DNA is bound to protein. A solution of unlabeled competitor DNA is then deposited on the gel surface and diffuses inside the porous matrix, establishing a concentration gradient $c(z, t)$ that changes over the z-position of the focal plane and time t (**Figure 1a**, **Figure 2a-2c**). The TF bound to the Cy5-reference DNA is thus locally exposed to different concentrations of the competitor DNA that competes for binding, leading to a dynamically changing FA of the Cy5-reference DNA $FA_{REF}(z, t)$ (**Figure 2b** and **2c**).

To determine the competitor concentration $c(z, t)$, we measure in separate wells (calibration wells) the dynamically changing FA signal of Nile Blue (NB) $FA_{NB}(z, t)$ (**Figure 2a** and **3**). This dye intercalates into DNA and thereby acts as a DNA sensor for the competitor DNA. With this controlled delivery system, tens to hundreds of different DNA-protein binding affinities can be

measured within one multi-well plate (96- or 384-well plate format). Measurement is then performed sequentially until complete displacement of the labeled reference DNA from the TF. We determined the binding specificity for a given factor by measuring the affinities of all 3 N single-base mutations of the consensus sequence of length N . HiP-FA requires low amounts of protein (\sim pmols per titration curve) and shows low variability in the determination of K_D s [coefficient of variation (CV) < 20%], while allowing measurements at a relatively large scale. The method can be conducted manually or fully automated using a robotic system, resulting in even lower CVs (**Figure 4**, upper panel). Dissociation constants are measured with high accuracy down to 0.5 nM. For extremely high affinities (K_D < 500pM), we use a standard competitive titration (**Figure 5**) due to the inaccuracies in measuring competitor DNA concentrations at low levels (< 100 nM).

HiP-FA can be implemented on nearly any standard, inverted, epifluorescence fluorescent microscope, provided the availability of an automated XY-stage and a piezo z-axis stage. Optical components were built around an automated widefield setup equipped with a long-distance objective. In practice, the assay can be adapted to objectives with other characteristics (in particular working distance and numerical aperture). However, this requires optimization of the parameters (distances between the z-slices, porosity and height of the agarose gel, etc.). The use of other kinds of lasers or camera is also possible. A detailed description of the entire experimental procedure and data analysis is given below in the protocol section.

PROTOCOL:

1 Polarization Microscopy

1.1 For widefield laser illumination, focus a 638 nm line of a continuous diode laser (40 mW) on the aperture of multimode optical fiber for beam cleanup. Mount a linear polarizer at the output of the fiber to set the polarization of laser light.

1.2 Block the excitation component of the emitted light with a dichroic mirror (640 nm cut-off) and a bandpass filter (bandpass 700/75).

1.3 Let the fluorescence signal pass through a polarizing beam splitter, which splits the emitted light into its perpendicular and parallel polarized components. Then, focus the non-reflected beam (parallel component) and the reflected beam (perpendicular component) with an achromatic lens of 200 mm focal length on the chip of a back-illuminated EM-CCD camera (**Figure 1b** and **1c**). Use a mirror to adjust the direction of the perpendicular beam toward the lens.

2 Design and Testing of Fluorescent-Labelled Reference DNA Oligomer

2.1 Determine the core sequence of the reference DNA: the method is based on a competitive assay that measures the dissociation constant (K_{D2}) between a transcription factor and unlabeled competitor DNA oligomer that competes for binding with a fluorescently labeled DNA whose affinity to the TF acts as a reference (K_{D1}). The consensus sequence obtained from other sources

like DNase footprinting or bacterial 1-hybrid can serve as a starting point^{5,15}.

NOTE: As a rule of thumb, a suitable reference DNA has a 3 to 7-fold decrease in binding affinity to the TF compared to the consensus sequence.

2.2 Measure by HiP-FA the K_{D1S} of 2-3 tentative single mutations of the consensus sequence derived in the previous step. Try to mutate positions in consensus sequence that are not too specific to avoid complete loss of binding.

NOTE: It is important that the reference sequence is bound by the transcription factor of interest (we used in this protocol Giant Gt), but not too strongly, so that weaker competitors can outcompete it at high concentrations.

2.3 Extend the core motif (8-12 base pairs generally) to a length of 16 base pairs or more by adding symmetrically flanking sequence at both sides (add side chains for proper binding). If necessary (for longer binding domains, for example), use longer sequences (up to ~50 base pairs in length were tested with the HiP-FA assay).

CAUTION: Be careful not to add bases that are expected to create ectopic binding sites. Use computational tools that predict binding sites from available PWMs to facilitate this process (e.g., PySite²²).

2.4 As labeled reference DNA, order oligomers that are fluorescently labeled on either forward or reverse strand at the 3' or 5' end. Use, for example Cy5, Bodipy-650 or any other suitable dye at a concentration of 10 μ M (100 μ M 10x stock) in water, and dilute stepwise as described in step 3.1.

2.5 Prepare 500 mL of 1x binding buffer by adding 33 mM potassium phosphate buffer (pH = 7.0), 90 mM NaCl, and 0.01% non-ionic detergent in distilled water. Also prepare 3x binding buffer, which contains the same components, except at threefold concentrations. If using 3x binding buffer as stock solution for the 1x binding buffer, prepare volumes > 500 mL; otherwise, prepare 250 mL.

NOTE: This composition was optimized for transcription factor stability and to prevent glutathione S-transferase (GST) dimerization.

2.6 Measure with the microscopy setup described in step 1 the FA of 200 μ L of binding buffer containing 0.8 nM labeled reference DNA in the presence of different amount of TF in a glass bottom microscopy 96-well plate (5-6 wells with different TF concentrations) to determine the TF concentration to use. Perform a titration series with increasing amounts of TF and choose for the assay the concentration for which the curve reaches a plateau, indicating complete binding of the DNA reference oligomer.

NOTE: The optimal TF concentration depends on the values of the TF-DNA dissociation constants.

Generally, lower K_{DS} require lower concentrations.

3 Oligomer Annealing

3.1. To anneal the DNA oligomers of the labeled reference DNA (sequence determined in the previous step), mix 7 μ L of a 10 mM dye-labeled forward single-stranded DNA solution and 7 μ L of a 10 mM concentration of its unlabeled reverse complement in 186 μ L of water.

3.2. For the competitor DNA sequences, mix 20 μ L of 100 mM solutions (in water, provided by the manufacturer) of forward single-stranded DNA with 20 μ L of 100 mM of the corresponding reverse single-stranded DNA for each individual competitor sequence to be measured.

3.3. Perform the annealing separately in a standard PCR cycler by heating up the solutions to 70 °C for 3 min and decreasing the temperature to RT at a rate of 0.1 K/s. If the PCR machine used does not support temperature gradients at that rate, simply do stepwise incubations with decreasing temperatures (tested were 99 cycles of 3 s with -0.4 K per cycle).

4 Gel Preparation

NOTE: The following section explains the preparation of two different kind of gels: 1) the titration wells contain gels with protein and are used to determine the K_{DS} for the respective competitor DNA sequences, and 2) the calibration wells make use of NB to determine the DNA concentration at every given time point and acquisition height. The focus is on the preparation of the experiment in a 96-well plate, but the corresponding volumes for a 384-well plate format are also indicated.

4.1 Dissolve 0.5% w/v low melting point agarose in the binding buffer by boiling it in a laboratory microwave oven. After complete dissolution, adjust the volume again with ddH₂O to compensate for possible evaporation.

NOTE: For convenience, prepare a stock of 10-20 10 mL aliquots of the gels and melt them at 75°C when they are needed. Gel stocks can be stored at RT.

CAUTION: Be careful to avoid superheating of the gel solution in the microwave oven. Short heating time intervals with shaking in between are preferable.

4.2 To prepare titration and calibration wells, first melt two 10 mL gel stock aliquots at 75 °C

under shaking.

4.2.1 Use 240 μ L (including 20% overhead) for each competitor (n = number of competitor sequences).

4.2.2 Use the same volume of gel for the NB calibration well to ensure an equal temperature and viscosity of both gels.

4.2.3 Then set the temperature to 35 $^{\circ}$ C and wait for the temperature to equilibrate.

4.3 For the titration wells, add 1.4 nM (final concentration) hybridized reference DNA (obtained in step 3), TF protein (final concentration C_{TF} = 20-60 nM, as determined in step 2.66), DTT (0.2 mM), and binding buffer in a total volume of $n \times 200 \mu$ L or $n \times 13 \mu$ L in a 96- or 384-well plate format, respectively (plus overhead). Mix thoroughly by inverting/shaking (do not vortex).

4.4 Slowly add 200 μ L per well in 96-well plate format (13 μ L/well for 386 wells) of the gel solution prepared in the previous step into the titration wells the well plate.

4.5 For the calibration wells, first add 5 nM NB to the melted gel outside the wells (total volume depending on the well plate format used and on the number of calibration wells; usually 5-6 per well plate is enough).

4.6 Pipette 200 μ L (13 μ L for 384-well plate format) of NB containing gel slowly within the titration wells of the well plate and make sure to avoid air bubbles.

NOTE: The usage of electronic pipets or robotics significantly increases reproducibility.

4.7 Let the gel solidify for 10 min at RT, and another 10 min at 4 $^{\circ}$ C (remove condensation from the glass afterwards if necessary). Make sure to conduct all these steps on a perfectly horizontal surface to avoid inhomogeneous gel surfaces.

NOTE: The protein containing gels are usually stable for at least several hours at 4 $^{\circ}$ C.

5 Adding the Competitor DNA Solution

NOTE: The following solutions should be prepared before starting the titration and are added on top of the calibration and titration wells simultaneously.

5.1 Add the annealed labeled reference DNA and protein in 3x binding buffer at 3 times higher

concentrations than the gel stock aliquots.

5.1.1 Mix 20 μ L of the obtained solution with 40 μ L of each annealed competitor DNA solution obtained in step 3.

5.1.2 For each calibration well, mix 20 μ L of 3x binding buffer containing 15 mM NB solution with 40 μ L of annealed competitor DNA (any sequence of the same length is suitable).

NOTE: For the 384-well plates, use 21 μ L instead of 60 μ L in total.

5.2 Optionally, check the homogeneity of the gel height levels in the different wells of the plate spectroscopically by measuring the absorbance at 380 nm, using a multi-well plate reader (the absorbance values are proportional to the gel heights).

5.3 Add 50 μ L (7 μ L for 384-well plate format) of the mixed competitor DNA solutions (annealed in step 3) on top of the gels. Try to add all the competitor solutions as simultaneously as possible by using electronic multichannel pipets or a 96-channel pipetting head, if available. After addition of the competitor solutions, place the plate on the microscope stage and start the measurements immediately (step 6).

6 Image Acquisition

6.1 Sequentially acquire times series of z-stacks (*e.g.*, use 12 planes and 100-300 ms of illumination time). Avoid taking images too close to the well surface ($< \sim 1.4 \mu$ m with the plates used herein) to exclude any polarization bias.

6.2 Perform 10-25 cycles of measurements until complete unbinding of the labeled reference DNA from the TF. The endpoint is typically reached after 1-2 h, depending on the binding kinetics and diffusivity of the competitor DNA.

7 Extraction of $FA(z,t)$ from Raw Data

7.1 Once a well plate has been imaged, compute from the raw fluorescence images the average pixel values of regions of interest for the parallel (I_{\parallel}) and perpendicularly (I_{\perp}) polarized intensity components (**Figure 1c**). This can be done automatically using the HiP-FA software²³.

NOTE: The HiP-FA software, an instruction manual, and a test dataset can be downloaded²³. Alternatively, use any other custom-written software to extract I_{\parallel} and I_{\perp} and perform the downstream analysis of the titration curves, as described in detail below.

7.2 Calculate FA for each well. For each well, the script computes $FA(z,t)$ at each z-position and time point t according to:

Equation 1:
$$FA(z,t) = \frac{I^{\parallel}(z,t) - G \cdot I^{\perp}(z,t)}{I^{\parallel}(z,t) + 2 \cdot I^{\perp}(z,t)}$$

Where G is the instrument G-factor that corrects for any bias toward the perpendicular channel.

7.3 Determine the G-factor of the microscopy setup by measuring the FA of any solutions containing a fluorescent dye of known anisotropy. Extract the two polarization components of the signal and then use Equation 1 to obtain G , knowing the FA of the solution ($G = 1.15$ in this setup).

8 Calibration Curve for Determination of Competitor DNA Concentration from FA_{NB}

8.1 Anneal 120 μ L of each forward and reverse reference oligomer (100 mM stock concentration; any random sequence with the same length as the competitor sequence can be used) and mix with 120 μ L of 3x binding buffer containing NB (15 nM).

8.2 Prepare a dilution series with 1:2 dilutions in 1x binding buffer with 6 dilutions in total. Mix 50 μ L of these dilutions with 200 μ L of 0.5% low melting point agarose ($T > 35$ °C) gel in 1x binding buffer containing 5 nM of NB in triplicates.

8.3 Add 200 μ L of each of the 6 solutions prepared in the previous step in a 96-well plate and store the plate for 1 h at 4 °C to ensure complete gelation, then 1 h at RT. Measure the FA_{NB} of the solutions by using the HiP-FA setup.

8.4 Extract $FA_{NB}(z,t)$ according to the previous step and fit the data using a Hill equation:

Equation 2:
$$FA(z,t) = \frac{FA_{max} \times c_{DNA}^n}{c_{DNA}^n + k^n}$$

Where C_{DNA} is the concentration of the DNA oligomer; k the concentration of the DNA oligomers at which half of the binding sites are occupied; FA_{max} is a normalization constant; and n is the Hill coefficient. k , FA_{max} , and n are set as free parameters during the fitting procedure.

8.5 Enter the three parameters obtained from the fitting procedure in the HiP-FA software (in the left lower panel).

8.6 Repeat the determination of the calibration curve every few months or after making changes in the microscopy setup.

9 Determination of Competitor DNA Concentrations

9.1 Use the HiP-FA software to extract $c(z,t)$ from the $FA_{NB}(z,t)$ measurements (**Figure 3**). First obtain the calibration curve as described in the previous section and enter the fitting parameters to the software (see manual for details).

9.2 Use the program to automatically extrapolate $c(z,t)$ for $c < 100$ nM (see manual for details) using Equation 3 (**Figure 3b**), which describes the one-dimensional diffusion of the

competitor DNA within the agarose gel matrix, assuming free diffusion.

Equation 3:

$$c(z, t) = C_0 \left(1 + \operatorname{erf} \left(\frac{-z}{\sqrt{4D(t+t_0)}} \right) \right)$$

Where C_0 is the initial concentration of the competitor DNA; erf is the error function; z is the position; D is the diffusion coefficient of the competitor DNA; and t_0 is the starting time of the measurements. The free parameters used are C_0 and z/\sqrt{D} .

10 Conventional Competitive Titration with HiP-FA for Very Strong DNA Binding

10.1 Serially dilute the different competitor DNA oligomers in the rows of a 96-well plate (or 384-well plate) at the concentrations of: 0, 1.25, 3.5, 9, 19, 45, 90, 190, 425, 900, 1900, and 4000 nM. Add the Cy5-labeled reference DNA (1 nM) and TF (20-50 nM) at a constant concentration, with a total volume of 200 μ L per well in binding buffer (**Figure 5a**). Wait 40 min until thermodynamic equilibrium is achieved and acquire (with the HiP-FA setup) z -stacks for each well (acquiring several images per well reduces variability by averaging the calculated FA values).

10.2 Construct the equilibrium binding titration curves and fit them with Equation 4 (**Figure 5b**). The K_D s determined by conventional competitive titration are identical to those obtained by HiP-FA using an agarose gel matrix²⁰.

11 Fitting Procedure of the FA Titration Curves

11.1 Display in the HiP-FA software the reconstructed titration curves for the individual competitor sequences $FA(z, t) = f[c(z, t)]$ and visually check the data quality (see manual for details). If needed, refine the parameters used for the determination of the competitor DNA concentrations in step 10.

11.2 Fit each individual titration curve automatically using Equation 4, which gives an analytical solution for competitive titration assays²⁴.

Equation 4:

$$FA = A \times \frac{2\sqrt{(d^2 - 3e)} \cos\left(\frac{\theta}{3}\right) - d}{3K_{D1} + 2\sqrt{(d^2 - 3e)} \cos\left(\frac{\theta}{3}\right) - d} + B$$

With:

$$\begin{aligned} d &= K_{D1} + K_{D2} + L_{ST} + L_T - R_T \\ e &= (L_T - R_T)K_{D1} + (L_{ST} - R_T)K_{D2} + K_{D1}K_{D2} \\ f &= -K_{D1}K_{D2}R_T \\ \theta &= \arccos\left(\frac{-2d^3 + 9de - 27f}{2\sqrt{(d^2 - 3e)^3}}\right) \end{aligned}$$

Where R_T is the protein concentration; L_T is the unlabeled and L_{ST} is the labeled DNA concentration; K_{D2} is the dissociation constant to be determined; R_T is the concentration of active protein; and A and B are normalization parameters.

First determine K_{D1} , which serves as a reference for the determination of the different K_{D2} values. K_{D1} can be readily determined with the assay by choosing the sequence of dye-reference DNA as the sequence of the unlabeled competitor DNA (see manual).

11.3 Enter the obtained value of K_{D1} in the software and compute the K_{D2} values for all the competitor DNA on the plate.

NOTE: The free parameters of the fitting procedure are K_{D2} , R_T , A , and B .

11.4 Export the dissociation constant K_{D2} and concentration of active protein R_T for all the individual titration wells of the plate by clicking the “Export” button in the software.

12 PWM Construction, Specificity of Protein-DNA Interaction, and Pseudo Counts

Create the sequence logos for the different PWMs using the online tool WebLogo 3.0 (<http://weblogo.threeplusone.com/create.cgi>) as described previously²⁰.

REPRESENTATIVE RESULTS:

We applied HiP-FA to TFs of the segmentation gene network^{25,26}, which generates the anterior-posterior body pattern of *Drosophila* embryos, largely through transcriptional regulation. From this network, we chose the bZIP domain TF Giant (Gt) for a detailed analysis (**Figure 4**). Since full-length transcription factors are difficult to express and yield mostly the same binding preferences as their DNA binding domains (DBD)¹³, we used the DBD fused to GST and expressed the construct in *E. coli* GST fusion proteins to deliver the same results as DBDs alone²⁰.

The Gt consensus sequence (**ATTACGTAAC**) represents the strongest binding sequence that we determined as described above. We then investigated the influence on the binding energy of all possible single-point mutations within the 10-mer Gt consensus sequence (a total of 30), flanked by additional bases at the 5' and 3' ends. We measured two replicates whose gel samples were produced using automation, and one additional replicate produced manually for comparison. The K_D s ranged from 0.6 to > 2000 nM for singly mutated sequences, and we also confirmed complete lack of binding to a “non-binding” sequence (data not shown).

TF-DNA binding specificities are typically modelled using a position weight matrix (PWM), in which a score is assigned to each possible nucleotide at each position in the binding motif. The PWM assumes that each position contributes to binding strength independently and in most cases constitutes a sufficient model for TF binding preferences²⁷. We generated revised PWMs based on our affinity measurements following established procedures^{28,29} and compared them to two PWMs previously reported in the literature. The first is based on nucleotide frequency

counts from binding sites identified by DNA footprinting^{4,5}, and the second PWM was obtained by bacterial one-hybrid (B1H) selection.¹⁵

The high similarity of the PWMs for the three replicates (**Figure 4**, upper panel), including for the sample prepared manually (replicate 3), demonstrates the high reproducibility of the HiP-FA method. While the PWMs obtained by HiP-FA are overall similar to the PWMs obtained with the other methods (**Figure 4**, lower panel), there are significant deviations: at position 2 (black arrow), the start of the core bZIP motif, mutations T>(G,C,A) lead to complete loss of binding in the motif obtained by HiP-FA, which is consistent with the B1H motif but not with that obtained with DNase footprinting, in which the binding remains relatively strong for bases (G,A). Conversely, at position 7 (gray arrow), the mutation T>C leads to much stronger binding than what was expected based on the previously measured PWMs.

Other deviations are subtler but no less important. Overall, the HiP-FA PWM is less specific than the other two, reflecting the fact that many mutations from the consensus still result in moderately strong binding. This can be quantified using the information content (IC). The IC is 11.5 bits for the HiP-FA matrix (average of the three replicates), compared to IC = 13.4 bits and 16.8 bits for the DNase footprinting and B1H matrices, respectively. Generally (though not universally), the PWMs obtained by HiP-FA are less specific than those obtained by other methods, based on 26 TFs investigated²⁰.

FIGURE AND TABLE LEGENDS:

Figure 1: Schematic depictions of the HIP-FA assay and experimental setup. (a) Gel delivery system for titrating competitor DNA in single wells. (b) HIP-FA microscopy setup. Customized automated widefield microscope with polarized fluorescence light detection on an EM-CCD camera. (c) Raw fluorescence image with the two regions of interest used to determine the parallel (red) and the perpendicularly (green) polarized components. (d) Typical layout of a 96-well plate.

Figure 2: Raw FA data and reconstructed titration curves. (a) Typical $FA(z,t)$ trajectory for a calibration well containing NB. (b,c) $FA(z,t)$ time trajectories for two titration wells measuring binding to a strong (b) and more moderate (c) DNA binding competitor. (d, e) Corresponding reconstructed FA titration measurements and fitted curves for the strong (d) and moderate (e) binding.

Figure 3: Determining the concentration of the competitor DNA $c(z,t)$ using Nile Blue (NB). (a) FA-concentration calibration curve for 16 base pairs DNA oligomers. In a conventional titration series, NB is embedded in agarose gel together with different concentrations of competitor DNA. The affinity of NB to DNA is sequence-independent²⁰; therefore, the same calibration curves can be used for determining $c(z,t)$ for different DNA sequences of the same length. (b) Competitor DNA time diffusion profile at an arbitrary z height determined using five calibration wells. For each measurement cycle, the average FAs of four NB-containing wells are displayed as white dots. The curves are fitted using Equation 3 (white line, individual wells in color) and the $c(z,t)$ at low concentrations ($C < \sim 100$ nM) is determined by the extrapolated fitting curve.

Figure 4: Binding specificities of the bZIP domain family TF Giant (Gt). HIP-FA PWMs of three replicates: two prepared using automation and one manually prepared (upper panel) are compared with PWMs generated by DNase footprinting and by the bacterial one-hybrid (B1H) selection method (lower panel). Overall, the HIP-FA binding motifs agree with previous data but also show significant differences, as highlighted with black and gray arrows.

Figure 5: Conventional competitive titration with HIP-FA. (a) Plate design shows 8 different competitor DNA serially diluted in binding buffer in a single row of a 96-well plate. An FA heat map is shown for different arbitrary binding strengths. (b) Competitive titration of three competitor DNAs binding to the Bcd TF with different affinities.

DISCUSSION:

HiP-FA is a comprehensive new method for determining the binding preference landscapes of TF-DNA interactions. It measures binding affinities of mutational DNA motif variants directly, avoiding any underlying assumption that binding preferences are reflected in the frequency of nucleotide occurrence in a set of above-threshold binders. Measurement takes place in the solution without immobilization and mechanical or chemical interference with the binding reaction, approximating equilibrium conditions as closely as possible. The controlled delivery system permits the measurement of a full titration curve within a single well and increases both throughput and reliability while saving protein. Using an objective with a high numerical aperture and EM-CCD camera with a high light collection efficiency allows for highly sensitive fluorescent light detection. Hence, with this setup, small FA changes as low as 10-15 mP can be accurately detected; in practice, this means that any binding reaction for which the mass increase after binding is minimal (as low as a mass ratio of 2) is readily detected. This is usually not the case with commercial systems like microplate readers. Due to its high sensitivity, HiP-FA extends the range of dissociation constants that can be measured reliably into the picomolar range. Binding energies are determined accurately over multiple orders of magnitude.

To evaluate the quality of the revised PWMs, we performed two types of analysis²⁰. We tested, for five factors of the segmentation gene network, how well different PWMs can predict experimental ChIP-seq profiles in the genomic regions of 21 segmentation genes. As a second test, we used a sequence-to-expression model⁴ that predicts expression patterns of segmentation enhancers on the basis of the binding preference and protein concentration of participating TFs. In both exercises, we found that the less specific HiP-FA PWMs perform significantly better than the more specific footprinting and B1H PWMs²⁰.

Unlike *de novo* methods, HiP-FA requires some prior knowledge of a given TF's binding preference. However, consensus sequences are known for many TFs, and many existing methods can supply them¹³⁻¹⁵. If needed, the true optimal binding sequence can be found iteratively.

We used DNA reference oligomers fluorescently labelled with Cy5 and Bodipy-650. These dyes have proven to perform well for FA measurements since the anisotropy of bound and unbound labelled-reference DNA were the largest among the different tested dyes. This ensures a

maximum dynamical range for the FA values. Generally, any fluorescent dye with a fluorescence lifetime ≥ 1 ns is likely to be suitable but needs to be tested first. If possible, it is advised to use dyes fluorescing in the near-IR range to minimize protein autofluorescence.

The most critical step of the experimental procedure is the pipetting of the gel into the well plates. Good reproducibility requires the gel volumes to be as uniform as possible. Changes in gel height are translated into changes of diffusivity for the competitive DNA oligomer, and thus in apparent changes of affinity when evaluating the data. This is the main source of variance in a technical replicate. The use of an electronic pipet or automation techniques improves reproducibility. Air bubbles within the gel can be avoided by slow and careful pipetting. It is also important to add the all competitor solutions on top of the titration wells with as little delay as possible. For best reproducibility, the whole process can be automated using a pipetting robot with heat incubators. A critical part for transferring the protocol to automation is the necessary optimization of incubator temperature and the incubation times. Make sure to find an optimal balance between the viscosity of the gel (*i.e.*, not too cold) and the stability of proteins (*i.e.*, not too hot). This depends both on the dispensing speed of the gels into the wells and stability of the protein used.

HiP-FA makes use of a controlled delivery system for the competitor DNA oligomers. To construct the titrations curves, it is necessary to determine the competitor DNA concentration $c(z,t)$ for each given z -position within the gel matrix and time point t . This is another critical step, since the determination of the K_{Ds} depends directly on $c(z,t)$. Calibration wells containing the NB dye as a sensor for DNA concentration are used for this purpose (**Figure 1d**, **Figure 2a**). Usually, 3-5 calibration wells containing NB per plate are sufficient. Before evaluating any HiP-FA experiment, a NB calibration curve should be constructed for the set-up by performing a conventional titration series of NB dissolved in the agarose gel with a competitor DNA of any sequence at different concentrations (**Figure 3a**), as explained in detail in step 8. In the case of very strong binding ($K_D < 500$ pM), the extrapolation used for determination of low concentrations of competitor DNA becomes limiting, since it is less accurate than a direct measurement. However, for TFs with such low K_{Ds} , the HiP-FA setup can be used to perform a conventional competitive titration in binding buffer without the use of an agarose gel matrix (**Figure 5**). For example, one full titration with 12 different concentrations of competitor DNA can be performed in a single row of a 96-well plate.

The controlled delivery system also requires fast TF-DNA binding kinetics and stable proteins, since the diffusion through the agarose gel is dynamical (although slow). Both properties can be tested directly with the HiP-FA setup by following, over time, the FA of the TFs of interest when bound to their respective fluorescently labeled reference DNA. We measured K_{ON} and K_{OFF} rates for the investigated factors and found them to be on the order of milliseconds to seconds²⁰, in accordance with other studies³⁰. This is sufficiently fast to ensure that measurements take place at equilibrium. In the case of other binding reactions with slower kinetics, the diffusivity of the competitor can be tuned by lowering its concentration or reducing gel pore size. In the case of the tested TFs, which all have fast T_{OFF} (\sim seconds), a total measurement time of about 1-2 h is sufficient to ensure thermodynamic equilibrium at each measurement.

Another potential issue related to the protein is the formation of protein aggregates that may alter FA measurements. The use of other buffer conditions containing different additives (like tensides) can prevent aggregate formation, if necessary.

We have worked under the linearity assumption of the PWM; however, HiP-FA can be scaled to include all possible di-nucleotide mutations of the consensus sequence. Finally, HiP-FA can be adapted to measure other types of binding interactions. The prerequisite is to have available a suitable reference molecule bound by the protein which can be fluorescently labeled. With the controlled delivery system, a concentration gradient can be generated for any kind of ligand; therefore, protein-protein and drug-protein interactions can be measured with similarly high fidelity and throughput.

ACKNOWLEDGMENTS:

We thank J. Müller for cDNA clones and members of the Gaul lab, in particular S. Bergelt, for valuable advice and spirited discussion. This work was supported by SFB 646, Regulatory Networks in Genome Expression and Maintenance (C.J., P.B.), the Center for Integrated Protein Science (U.G.) and the Graduate School for Quantitative Biosciences Munich (M.S.). U.G. acknowledges support by the Deutsche Forschungsgemeinschaft (SFB 646, SFB 1064, CIPSM, QBM), the Bundesministerium für Bildung und Forschung (BMBF: ebio - Innovationswettbewerb Systembiologie), and the Humboldt-Foundation (Alexander von Humboldt, Professorship).

DISCLOSURES:

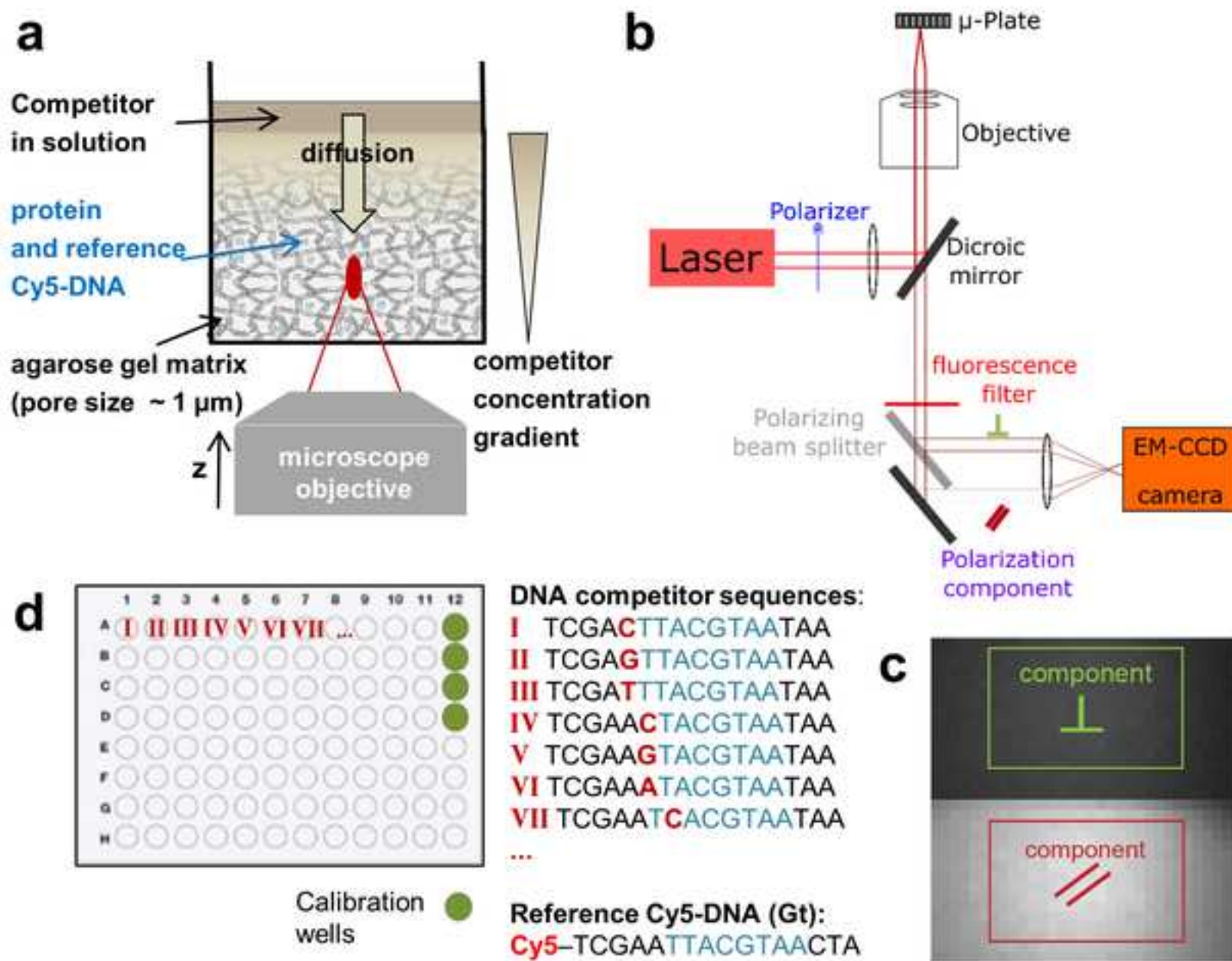
The authors declare no conflict of interests.

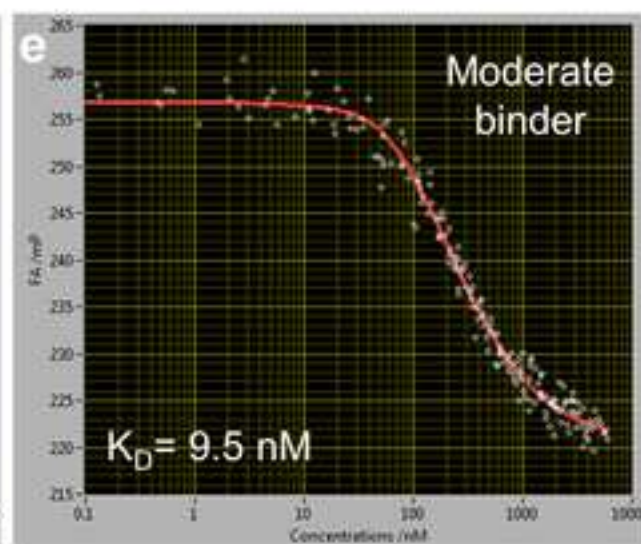
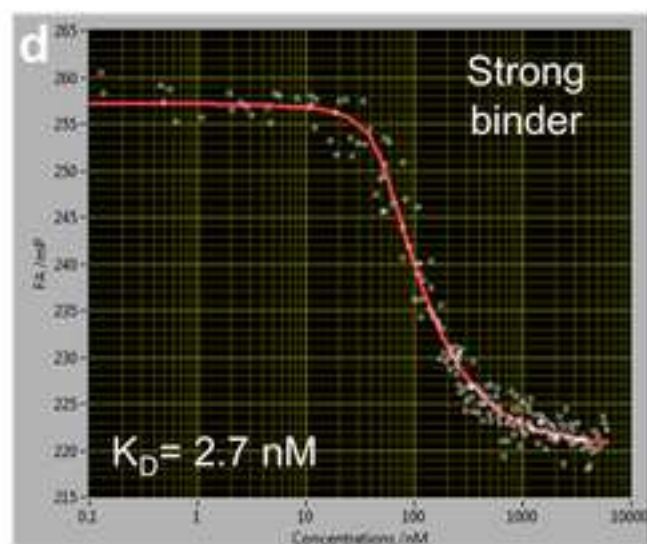
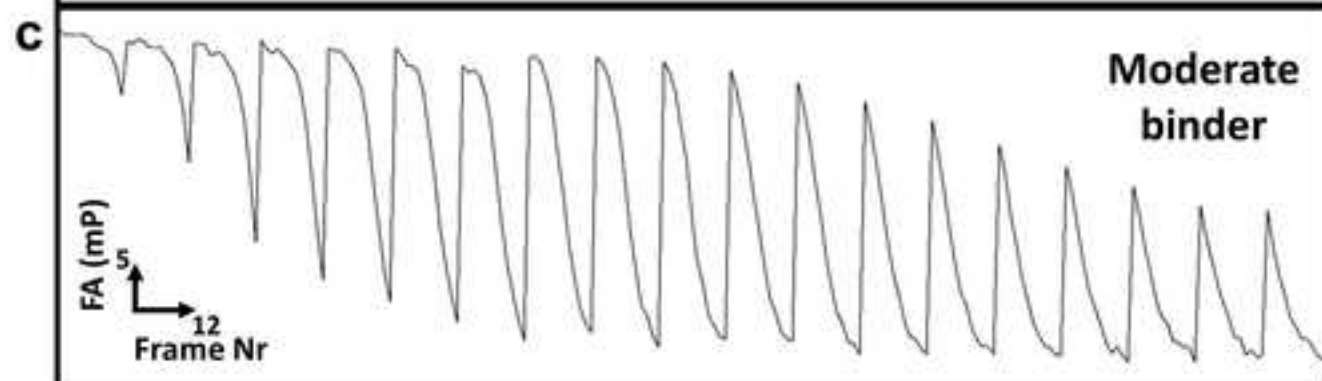
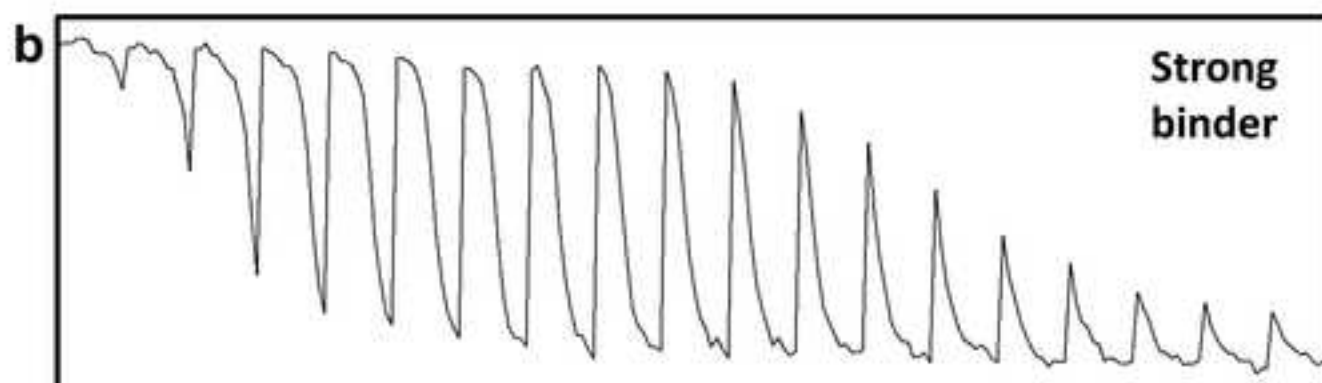
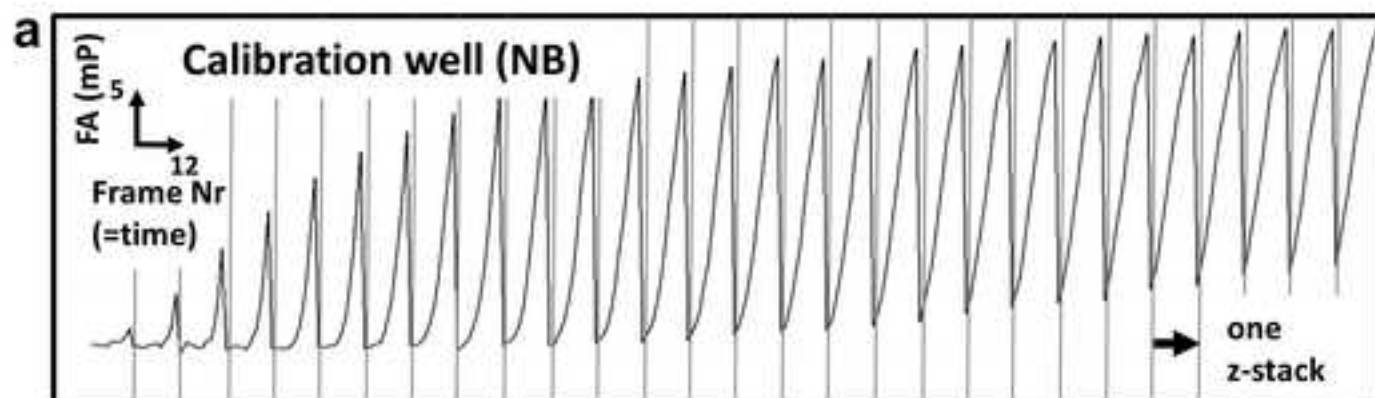
REFERENCES:

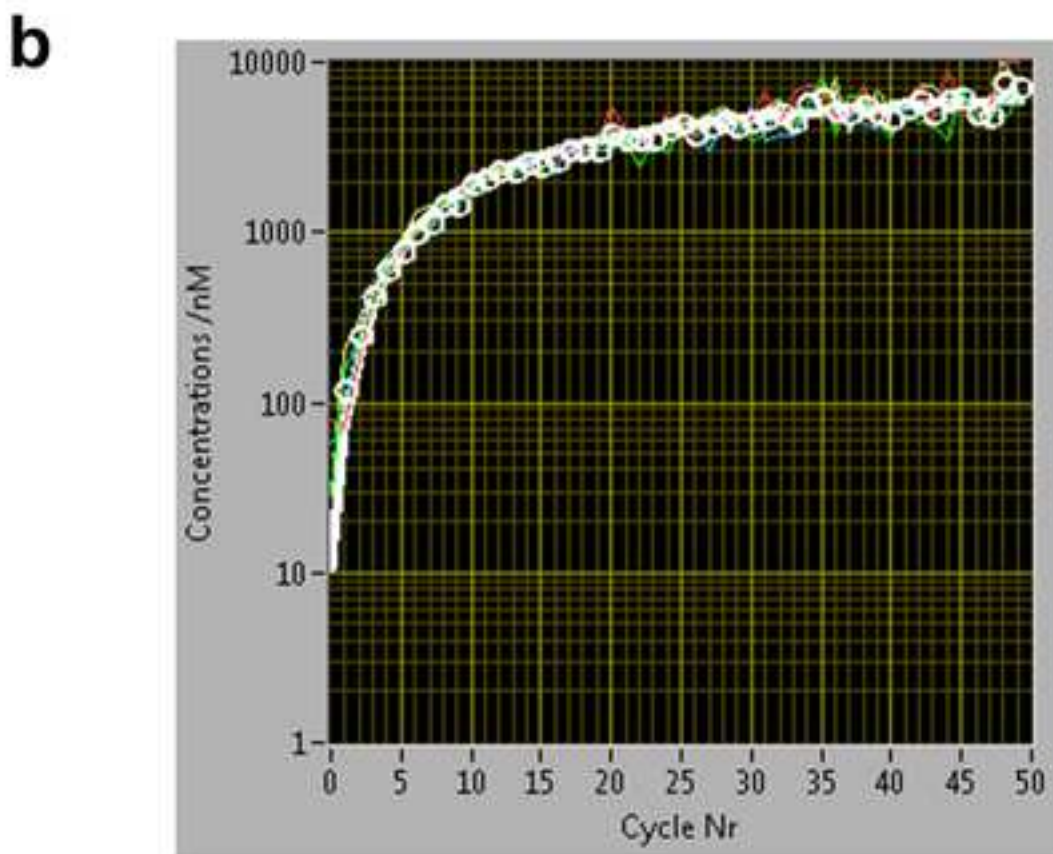
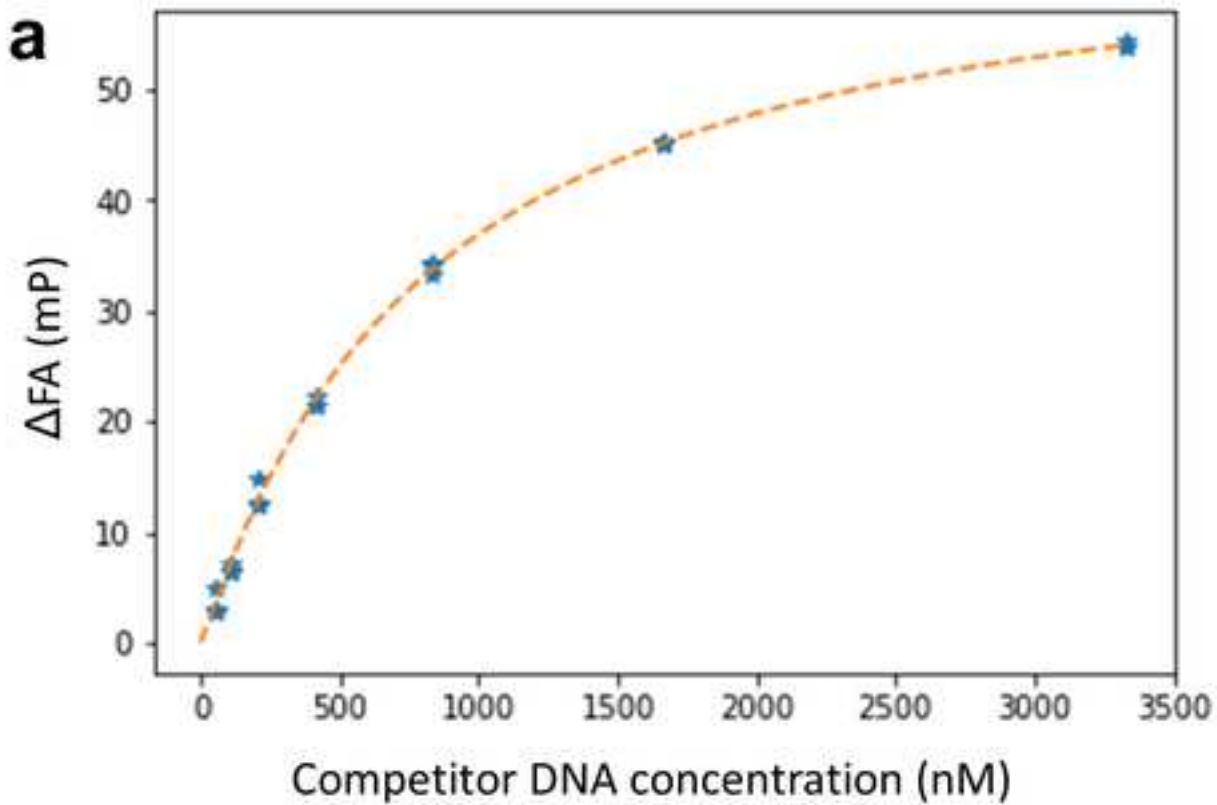
1. Berg, O. G., von Hippel, P. H. Selection of DNA binding sites by regulatory proteins. Statistical-mechanical theory and application to operators and promoters. *Journal of Molecular Biology*. **193**, 723-750 (1987).
2. Hammar, P., *et al.* Direct measurement of transcription factor dissociation excludes a simple operator occupancy model for gene regulation. *Nature Genetics*. **46**, 405-408 (2014).
3. Chen, J., *et al.* Single-molecule dynamics of enhanceosome assembly in embryonic stem cells. *Cell*. **156**, 1274-1285 (2014).
4. Segal, E., Raveh-Sadka, T., Schroeder, M., Unnerstall, U., Gaul, U. Predicting expression patterns from regulatory sequence in *Drosophila* segmentation. *Nature*. **451**, 535-540 (2008).
5. Schroeder, M. D., *et al.* Transcriptional control in the segmentation gene network of *Drosophila*. *PLoS Biology*. **2**, E271 (2004).
6. He, X., Samee, M. A., Blatti, C., Sinha, S. Thermodynamics-based models of transcriptional regulation by enhancers: the roles of synergistic activation, cooperative binding and short-range repression. *PLoS Computational Biology*. **6**, (2010).
7. Wilson, M.D., *et al.* Species-Specific Transcription in Mice Carrying Human Chromosome 21. *Science*. **322**, 434-438 (2008).
8. Galas, D. J., Schmitz, A. Dnaase footprinting - simple method for detection of protein-DNA

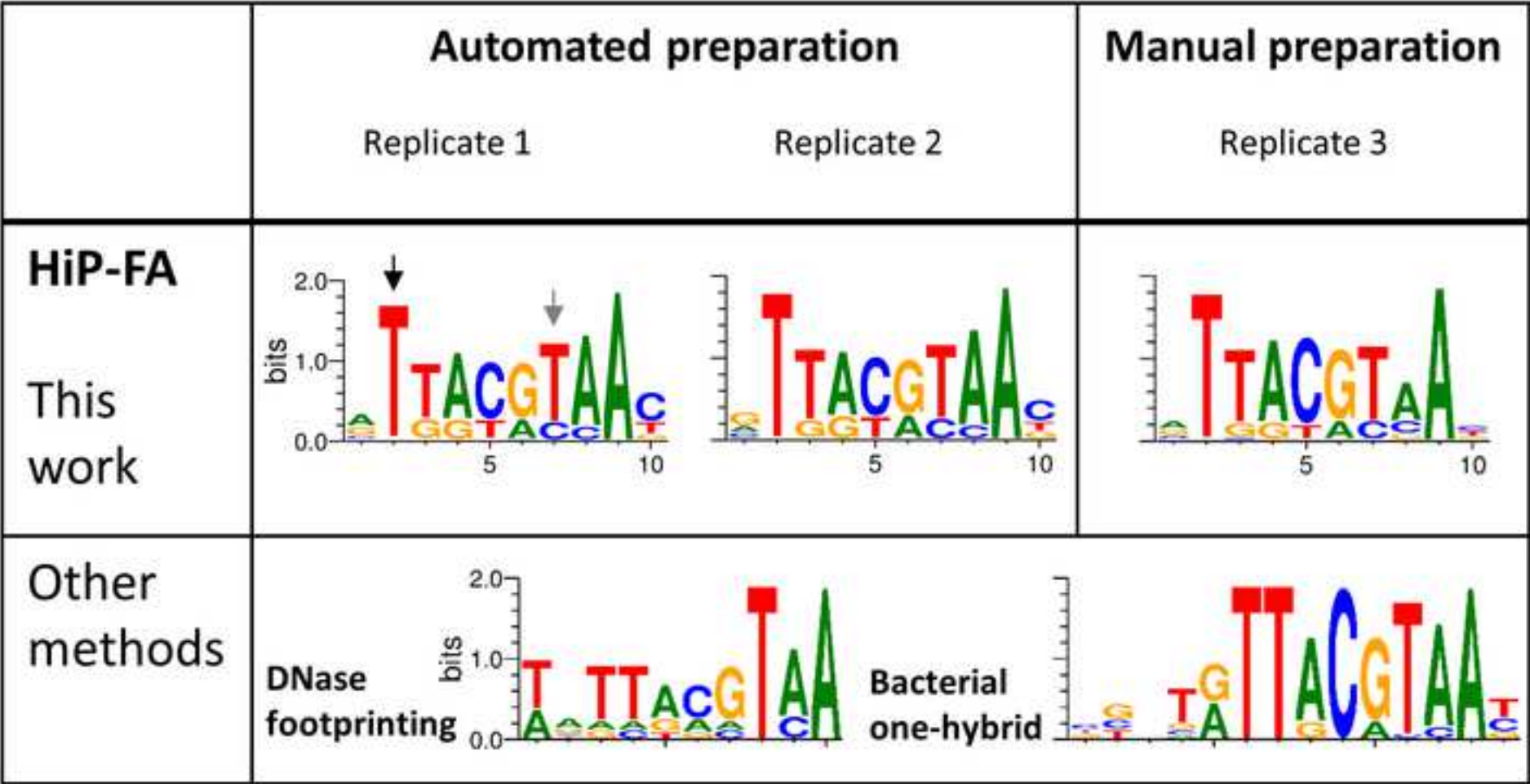
- binding specificity. *Nucleic Acids Research*. **5**, 3157-3170 (1978).
9. Hellman, L. M., Fried, M. G. Electrophoretic mobility shift assay (EMSA) for detecting protein-nucleic acid interactions. *Nature Protocols*. **2**, 1849-1861 (2007).
10. Liedberg, B., Nylander, C., Lundstrom, I. Surface-plasmon resonance for gas-detection and biosensing. *Sensors and Actuators*. **4**, 299-304 (1983).
11. Wienken, C. J., Baaske, P., Rothbauer, U., Braun, D., Duhr, S. Protein-binding assays in biological liquids using microscale thermophoresis. *Nature Communications*. **1**, (2010).
12. Berger, M.F., et al. Compact, universal DNA microarrays to comprehensively determine transcription-factor binding site specificities. *Nature Biotechnology*. **24**, 1429-1435 (2006).
13. Nitta, K.R., et al. Conservation of transcription factor binding specificities across 600 million years of bilateria evolution. *eLife*. **4**, (2015).
14. Jolma, A., et al. DNA-Binding Specificities of Human Transcription Factors. *Cell*. **152**, 327-339 (2013).
15. Noyes, M.B., et al. A systematic characterization of factors that regulate Drosophila segmentation via a bacterial one-hybrid system. *Nucleic Acids Research*. **36**, 2547-2560 (2008).
16. Nutiu, R., et al. Direct measurement of DNA affinity landscapes on a high-throughput sequencing instrument. *Nature Biotechnology*. **29**, 659-U146 (2011).
17. Riley, T.R., et al. SELEX-seq: a method for characterizing the complete repertoire of binding site preferences for transcription factor complexes. *Methods Molecular Biology*. **1196**, 255-278 (2014).
18. Maerkl, S. J., Quake, S. R. A systems approach to measuring the binding energy landscapes of transcription factors. *Science*. **315**, 233-237 (2007).
19. Isakova, A., et al. SMiLE-seq identifies binding motifs of single and dimeric transcription factors. *Nature Methods*. **14**, 316-322 (2017).
20. Jung, C., et al. True equilibrium measurement of transcription factor-DNA binding affinities using automated polarization microscopy. *Nature Communications*. **9**, 1605 (2018).
21. Weber, G. Polarization of the fluorescence of macromolecules: Fluorescent conjugates of ovalbumin and bovine serum albumin. *Biochemical Journal*. **51**, 155-168 (1952).
22. <https://github.com/Reutern/PySite>.
23. <https://github.com/GeneCenterMunich/HiP-FA>.
24. Roehrl, M. H., Wang, J. Y., Wagner, G. A general framework for development and data analysis of competitive high-throughput screens for small-molecule inhibitors of protein-protein interactions by fluorescence polarization. *Biochemistry*. **43**, 16056-16066 (2004).
25. St Johnston, D., Nusslein-Volhard, C. The origin of pattern and polarity in the Drosophila embryo. *Cell*. **68**, 201-220 (1992).
26. Pankratz, M., Jäckle, H. in *The Development of Drosophila melanogaster*, Vol. 1. (eds. M. Bate, A. Martinez Arias) 467-516 (Cold Spring Harbor Laboratory Press, Cold Spring Harbor; 1993).
27. Zhao, Y., Ruan, S. X., Pandey, M., Stormo, G. D. Improved Models for Transcription Factor Binding Site Identification Using Nonindependent Interactions. *Genetics*. **191**, 781-U204 (2012).

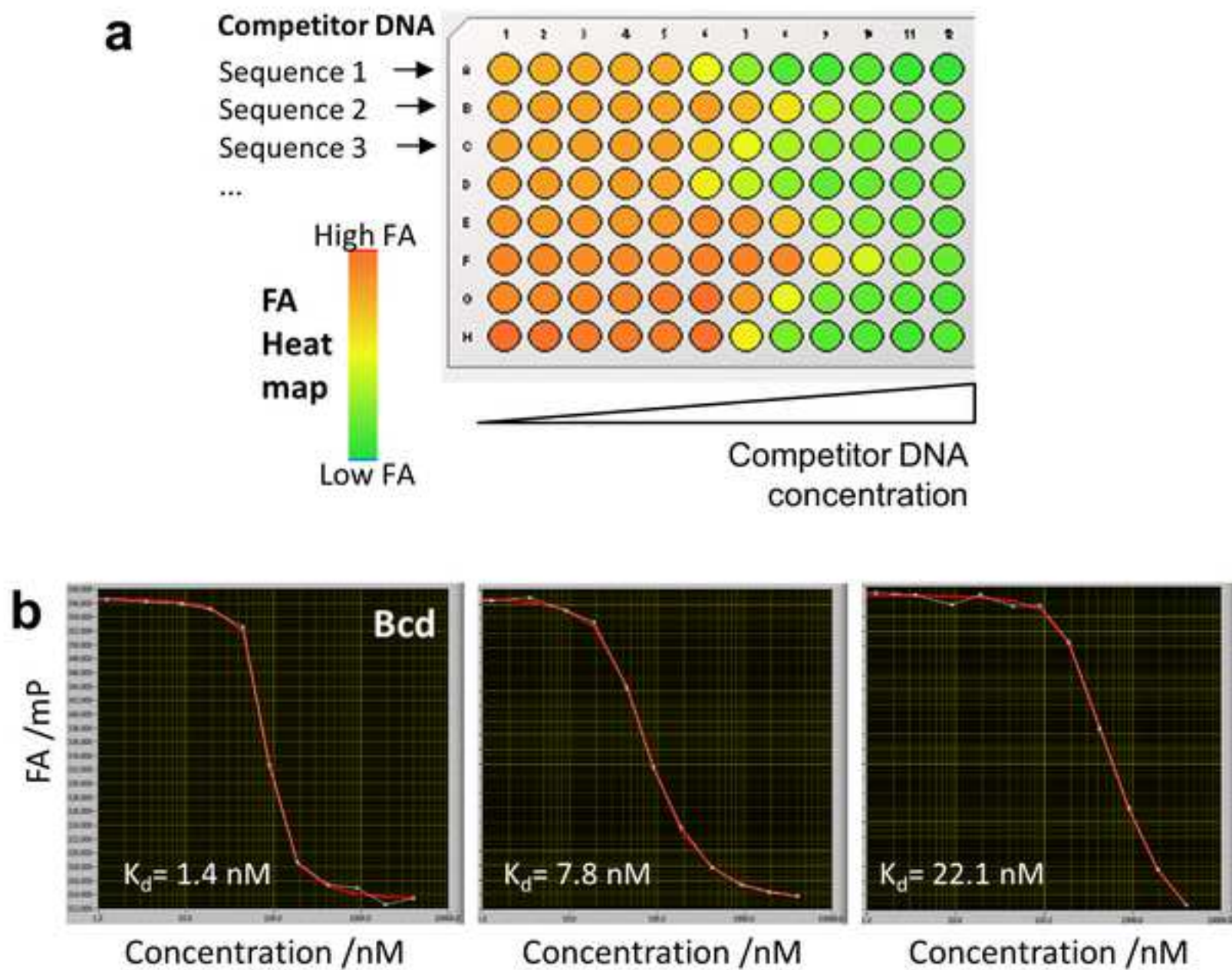
- 682 28. Nouredine, M.A., *et al.* Probing the functional impact of sequence variation on p53-DNA
683 interactions using a novel microsphere assay for protein-DNA binding with human cell
684 extracts. *PLoS Genetics*. **5**, e1000462 (2009).
- 685 29. Veprintsev, D. B., Fersht, A. R. Algorithm for prediction of tumour suppressor p53 affinity
686 for binding sites in DNA. *Nucleic Acids Research*. **36**, 1589-1598 (2008).
- 687 30. Geertz, M., Shore, D., Maerkl, S. J. Massively parallel measurements of molecular
688 interaction kinetics on a microfluidic platform. *Proceedings of the National Academy of*
689 *Sciences*. **109**, 16540-16545 (2012).
- 690











Name of Material/ Equipment	Company
Cy5-labeled 16- / 18-bp DNA-oligomers	Eurofins
16- / 18-bp DNA-oligomers	Eurofins
Nile Blue A	Sigma
Sensoplate plus microplate 96- or 384-well, PS	Greiner
384 Well Sensoplate, black	Greiner
Agarose, low gelling temperature	Sigma
Sodium Chloride	Merck
Tween-20	Sigma
Di-Potassium hydrogen phosphate trihydrate	Merck
Potassium dihydrogen phosphate	Merck
Q-POD Element	Merck Millipore
Millipak 40 Gamma Gold Filter	Merck Millipore
Milli-Q Integral 3 Water Purification System	Merck Millipore
Quantum TIX	Merck Millipore
DL-Dithiothreitol	Sigma
Mastercycler gradient	Eppendorf
SafeSeal tube 1.5 mL	Sarstedt
Tube 15 mL	Sarstedt
Multiply-Pro cup 0.2 mL PP	Sarstedt

MICROSCOPY SETUP:

Automated widefield microscope	LEICA
Long distance objective	LEICA
638 nm line continuous diode laser	Omicron
Back-illuminated EM-CCD Camera	Andor
Dichroic mirror	AHF
Bandpass filter	AHF
Linear polarizer	Thorlabs
Polarizing beam splitter	Thorlabs
Achromatic lens	Thorlabs
Multimode optical fiber	Optronis

ROBOTIC SYSTEM:

Our robotic system includes a Biomek NXP workstations with a 96-channel head and with Span-8 pipettors, connected with a servo-shuttle, are used for all liquid transfer steps. In addition, the system is equipped with orbital shakers and a microplate reader (Paradigm, Molecular device) served by the Span-8 gripper

Beckman Coulter

SOFTWARE:

Programming language	National Instruments
----------------------	----------------------

Script for the HiP-FA software available at

Catalog Number	Comments/Description
	Custom synthesis
	Custom synthesis
N5632-25G	
655891	175 µm thick glass bottom
788896	
A9414-50G	
1.06404.1000	
P1379-1L	
1.05099.1000	
1.04873.1000	
ZMQSP0DE1	
MPGL04GK2	
ZRXQ003WW	
QTUMOTIX1	
43815-1G	
Z316083	
72.706.200	
62.554.502	
72.737.002	
DMI6000	
HCX PL FLUOAR L 60x/0.60 N.A. Dry	
PHOxX 638-40, 40mW	
iXon DV897	
640nm cut-off	
ET bandpass 700/75	
LPVISC050-MP2	
BS010	
200 mm focal length	
FVP600660710	
Biomek NXP	
Labview 9.0	

<https://github.com/GeneCenterMunich/HiP-FA>

ARTICLE AND VIDEO LICENSE AGREEMENT

Title of Article:

High Sensitivity measurement of transcription factor-DNA binding energies by automated fluorescence microscopy

Author(s):

Jung, C., Schnepf, M., Bandilla, P., Unnerstall U., Gaul, U.

Item 1: The Author elects to have the Materials be made available (as described at <http://www.jove.com/publish>) via:

☐

Standard Access

☒

Open Access

Item 2: Please select one of the following items:

☒

The Author is **NOT** a United States government employee.

☐

The Author is a United States government employee and the Materials were prepared in the course of his or her duties as a United States government employee.

☐

The Author is a United States government employee but the Materials were NOT prepared in the course of his or her duties as a United States government employee.

ARTICLE AND VIDEO LICENSE AGREEMENT

1. **Defined Terms.** As used in this Article and Video License Agreement, the following terms shall have the following meanings: **"Agreement"** means this Article and Video License Agreement; **"Article"** means the article specified on the last page of this Agreement, including any associated materials such as texts, figures, tables, artwork, abstracts, or summaries contained therein; **"Author"** means the author who is a signatory to this Agreement; **"Collective Work"** means a work, such as a periodical issue, anthology or encyclopedia, in which the Materials in their entirety in unmodified form, along with a number of other contributions, constituting separate and independent works in themselves, are assembled into a collective whole; **"CRC License"** means the Creative Commons Attribution-Non Commercial-No Derivs 3.0 Unported Agreement, the terms and conditions of which can be found at: <http://creativecommons.org/licenses/by-nc-nd/3.0/legalcode>; **"Derivative Work"** means a work based upon the Materials or upon the Materials and other pre-existing works, such as a translation, musical arrangement, dramatization, fictionalization, motion picture version, sound recording, art reproduction, abridgment, condensation, or any other form in which the Materials may be recast, transformed, or adapted; **"Institution"** means the institution, listed on the last page of this Agreement, by which the Author was employed at the time of the creation of the Materials; **"JoVE"** means MyJoVE Corporation, a Massachusetts corporation and the publisher of The Journal of Visualized Experiments; **"Materials"** means the Article and / or the Video; **"Parties"** means the Author and JoVE; **"Video"** means any video(s) made by the Author, alone or in conjunction with any other parties, or by JoVE or its affiliates or agents, individually or in collaboration with the Author or any other parties, incorporating all or any portion

of the Article, and in which the Author may or may not appear.

2. **Background.** The Author, who is the author of the Article, in order to ensure the dissemination and protection of the Article, desires to have the JoVE publish the Article and create and transmit videos based on the Article. In furtherance of such goals, the Parties desire to memorialize in this Agreement the respective rights of each Party in and to the Article and the Video.

3. **Grant of Rights in Article.** In consideration of JoVE agreeing to publish the Article, the Author hereby grants to JoVE, subject to **Sections 4** and **7** below, the exclusive, royalty-free, perpetual (for the full term of copyright in the Article, including any extensions thereto) license (a) to publish, reproduce, distribute, display and store the Article in all forms, formats and media whether now known or hereafter developed (including without limitation in print, digital and electronic form) throughout the world, (b) to translate the Article into other languages, create adaptations, summaries or extracts of the Article or other Derivative Works (including, without limitation, the Video) or Collective Works based on all or any portion of the Article and exercise all of the rights set forth in (a) above in such translations, adaptations, summaries, extracts, Derivative Works or Collective Works and (c) to license others to do any or all of the above. The foregoing rights may be exercised in all media and formats, whether now known or hereafter devised, and include the right to make such modifications as are technically necessary to exercise the rights in other media and formats. If the "Open Access" box has been checked in **Item 1** above, JoVE and the Author hereby grant to the public all such rights in the Article as provided in, but subject to all limitations and requirements set forth in, the CRC License.

ARTICLE AND VIDEO LICENSE AGREEMENT

4. **Retention of Rights in Article.** Notwithstanding the exclusive license granted to JoVE in **Section 3** above, the Author shall, with respect to the Article, retain the non-exclusive right to use all or part of the Article for the non-commercial purpose of giving lectures, presentations or teaching classes, and to post a copy of the Article on the Institution's website or the Author's personal website, in each case provided that a link to the Article on the JoVE website is provided and notice of JoVE's copyright in the Article is included. All non-copyright intellectual property rights in and to the Article, such as patent rights, shall remain with the Author.

5. **Grant of Rights in Video – Standard Access.** This **Section 5** applies if the "Standard Access" box has been checked in **Item 1** above or if no box has been checked in **Item 1** above. In consideration of JoVE agreeing to produce, display or otherwise assist with the Video, the Author hereby acknowledges and agrees that, Subject to **Section 7** below, JoVE is and shall be the sole and exclusive owner of all rights of any nature, including, without limitation, all copyrights, in and to the Video. To the extent that, by law, the Author is deemed, now or at any time in the future, to have any rights of any nature in or to the Video, the Author hereby disclaims all such rights and transfers all such rights to JoVE.

6. **Grant of Rights in Video – Open Access.** This **Section 6** applies only if the "Open Access" box has been checked in **Item 1** above. In consideration of JoVE agreeing to produce, display or otherwise assist with the Video, the Author hereby grants to JoVE, subject to **Section 7** below, the exclusive, royalty-free, perpetual (for the full term of copyright in the Article, including any extensions thereto) license (a) to publish, reproduce, distribute, display and store the Video in all forms, formats and media whether now known or hereafter developed (including without limitation in print, digital and electronic form) throughout the world, (b) to translate the Video into other languages, create adaptations, summaries or extracts of the Video or other Derivative Works or Collective Works based on all or any portion of the Video and exercise all of the rights set forth in (a) above in such translations, adaptations, summaries, extracts, Derivative Works or Collective Works and (c) to license others to do any or all of the above. The foregoing rights may be exercised in all media and formats, whether now known or hereafter devised, and include the right to make such modifications as are technically necessary to exercise the rights in other media and formats. For any Video to which this **Section 6** is applicable, JoVE and the Author hereby grant to the public all such rights in the Video as provided in, but subject to all limitations and requirements set forth in, the CRC License.

7. **Government Employees.** If the Author is a United States government employee and the Article was prepared in the course of his or her duties as a United States government employee, as indicated in **Item 2** above, and any of the licenses or grants granted by the Author hereunder exceed the scope of the 17 U.S.C. 403, then the rights granted hereunder shall be limited to the maximum

rights permitted under such statute. In such case, all provisions contained herein that are not in conflict with such statute shall remain in full force and effect, and all provisions contained herein that do so conflict shall be deemed to be amended so as to provide to JoVE the maximum rights permissible within such statute.

8. **Protection of the Work.** The Author(s) authorize JoVE to take steps in the Author(s) name and on their behalf if JoVE believes some third party could be infringing or might infringe the copyright of either the Author's Article and/or Video.

9. **Likeness, Privacy, Personality.** The Author hereby grants JoVE the right to use the Author's name, voice, likeness, picture, photograph, image, biography and performance in any way, commercial or otherwise, in connection with the Materials and the sale, promotion and distribution thereof. The Author hereby waives any and all rights he or she may have, relating to his or her appearance in the Video or otherwise relating to the Materials, under all applicable privacy, likeness, personality or similar laws.

10. **Author Warranties.** The Author represents and warrants that the Article is original, that it has not been published, that the copyright interest is owned by the Author (or, if more than one author is listed at the beginning of this Agreement, by such authors collectively) and has not been assigned, licensed, or otherwise transferred to any other party. The Author represents and warrants that the author(s) listed at the top of this Agreement are the only authors of the Materials. If more than one author is listed at the top of this Agreement and if any such author has not entered into a separate Article and Video License Agreement with JoVE relating to the Materials, the Author represents and warrants that the Author has been authorized by each of the other such authors to execute this Agreement on his or her behalf and to bind him or her with respect to the terms of this Agreement as if each of them had been a party hereto as an Author. The Author warrants that the use, reproduction, distribution, public or private performance or display, and/or modification of all or any portion of the Materials does not and will not violate, infringe and/or misappropriate the patent, trademark, intellectual property or other rights of any third party. The Author represents and warrants that it has and will continue to comply with all government, institutional and other regulations, including, without limitation all institutional, laboratory, hospital, ethical, human and animal treatment, privacy, and all other rules, regulations, laws, procedures or guidelines, applicable to the Materials, and that all research involving human and animal subjects has been approved by the Author's relevant institutional review board.

11. **JoVE Discretion.** If the Author requests the assistance of JoVE in producing the Video in the Author's facility, the Author shall ensure that the presence of JoVE employees, agents or independent contractors is in accordance with the relevant regulations of the Author's institution. If more than one author is listed at the beginning of this Agreement, JoVE may, in its sole

ARTICLE AND VIDEO LICENSE AGREEMENT

discretion, elect not take any action with respect to the Article until such time as it has received complete, executed Article and Video License Agreements from each such author. JoVE reserves the right, in its absolute and sole discretion and without giving any reason therefore, to accept or decline any work submitted to JoVE. JoVE and its employees, agents and independent contractors shall have full, unfettered access to the facilities of the Author or of the Author's institution as necessary to make the Video, whether actually published or not. JoVE has sole discretion as to the method of making and publishing the Materials, including, without limitation, to all decisions regarding editing, lighting, filming, timing of publication, if any, length, quality, content and the like.

12. **Indemnification.** The Author agrees to indemnify JoVE and/or its successors and assigns from and against any and all claims, costs, and expenses, including attorney's fees, arising out of any breach of any warranty or other representations contained herein. The Author further agrees to indemnify and hold harmless JoVE from and against any and all claims, costs, and expenses, including attorney's fees, resulting from the breach by the Author of any representation or warranty contained herein or from allegations or instances of violation of intellectual property rights, damage to the Author's or the Author's institution's facilities, fraud, libel, defamation, research, equipment, experiments, property damage, personal injury, violations of institutional, laboratory, hospital, ethical, human and animal treatment, privacy or other rules, regulations, laws, procedures or guidelines, liabilities and other losses or damages related in any way to the submission of work to JoVE, making of videos by JoVE, or publication in JoVE or elsewhere by JoVE. The Author shall be responsible for, and shall hold JoVE harmless from, damages caused by lack of sterilization, lack of cleanliness or by contamination due to

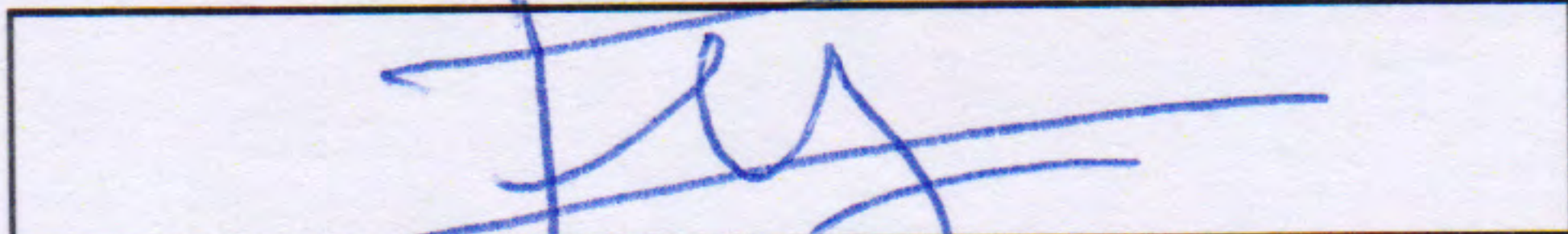
the making of a video by JoVE its employees, agents or independent contractors. All sterilization, cleanliness or decontamination procedures shall be solely the responsibility of the Author and shall be undertaken at the Author's expense. All indemnifications provided herein shall include JoVE's attorney's fees and costs related to said losses or damages. Such indemnification and holding harmless shall include such losses or damages incurred by, or in connection with, acts or omissions of JoVE, its employees, agents or independent contractors.

13. **Fees.** To cover the cost incurred for publication, JoVE must receive payment before production and publication the Materials. Payment is due in 21 days of invoice. Should the Materials not be published due to an editorial or production decision, these funds will be returned to the Author. Withdrawal by the Author of any submitted Materials after final peer review approval will result in a US\$1,200 fee to cover pre-production expenses incurred by JoVE. If payment is not received by the completion of filming, production and publication of the Materials will be suspended until payment is received.

14. **Transfer, Governing Law.** This Agreement may be assigned by JoVE and shall inure to the benefits of any of JoVE's successors and assignees. This Agreement shall be governed and construed by the internal laws of the Commonwealth of Massachusetts without giving effect to any conflict of law provision thereunder. This Agreement may be executed in counterparts, each of which shall be deemed an original, but all of which together shall be deemed to me one and the same agreement. A signed copy of this Agreement delivered by facsimile, e-mail or other means of electronic transmission shall be deemed to have the same legal effect as delivery of an original signed copy of this Agreement.

A signed copy of this document must be sent with all new submissions. Only one Agreement is required per submission.

CORRESPONDING AUTHOR

Name:	JUNG CHRISTOPHE	
Department:	GENE CENTER	
Institution:	LMU MUNICH	
Title:	Dr.	
Signature:		Date: 11/07/2018

Please submit a **signed** and **dated** copy of this license by one of the following three methods:

1. Upload an electronic version on the JoVE submission site
2. Fax the document to +1.866.381.2236
3. Mail the document to JoVE / Attn: JoVE Editorial / 1 Alewife Center #200 / Cambridge, MA 02140

LMU · Department für Biochemie · Butenandtstr. 1 · D-81377 München

JoVE

Dr Christophe Jung

Telefon +49 (0)89 2180-71101

Telefax +49 (0)89 2180-71104

jung@genzentrum.lmu.de

BioSyM /Genecenter

AG Prof. Gaul

Butenandtstr. 1

D-81377 München

Germany

Munich, 12.10.2018

Dear Dr Bajaj,

We are resubmitting our revised article JoVE58763R1 "High sensitivity measurement of transcription factor-DNA binding energies by automated fluorescence microscopy". The HiP-FA software have already a GUI. A description of the software and how to use it in details is provided in the Documentation file "HiP-FA Software_Documentation.docx" at: <https://github.com/GeneCenterMunich/HiP-FA> (Documentation File also provided in this submission as "HiP-FA Software_Documentation.docx" file). We didn't include additional steps on how to use the software since we feel that the Documentation covers it already, and that including it within the text would be too long and beyond the scope of this protocol.

We are looking forward to your response.

Sincerely Yours,

Ch. Jung

HiP-FA / Supplementary Software

The HiP-FA software is written in *Labview 9.0*. Open the “HiP-FA Software” script which appears on the top-level of the “HiP-FA_Labview9.0” library. The interface consists of six different modules: FILE, SETTINGS, ROIs, DNA CONCENTRATIONS, and TITRATION CURVES.

FILE. After starting the program, two different file paths are expected: first the raw data which are the raw images acquired with the camera converted into individual ASCII files. For example, the file name “044_I49_z11_ch00.txt”, where “044” is the well number, “I49” the 49th cycle of acquisition, and “Z11” the z-slice number. Select the file corresponding to the very last image acquired i.e. highest well, cycle and z-slice numbers (“044_I49_z11_ch00.txt” in the “Sequence” folder of the exemplary dataset provided.

“20140703_pdm2_Robot_Matrix_dupl1”). Select then a second file containing the numbers of the wells containing the Nile Blue (NB) intercalating dye embedded in agarose which serves as reference to determine the DNA concentrations $c(z,t)$. It should be a text file containing the list of the wells (see “Calibration_Wells.txt”). The loading of the data can be monitored in the FILE panel. The data, consisting of the two polarization components, can be flipped vertically if necessary by activating the “Flip data” switch. The loading of the data can be deactivated after re-starting the scripSpt to save time by switching the “Load Data” button to OFF.

SETTINGS. The SETTINGS panel is used to set the G factor (gfactor), the concentration of the labelled-DNA reference oligomer (Conc. DNA), the K_D of this sequence (K_{D1} , as determined by the titration of the same sequence as competitor DNA). In addition, the user can specify from which cycle number the data should be analyzed (Cycle Start), the number of cycles and of slices per z-stack to be analyzed (Nr Cycles and Nr slices, respectively), if it is desirable to analyze only a sub-fraction of the data (most of the information is contained in the firsts 10-20 cycles). “X(raw)” and “z” are used to change the well number and the z-height for the display in panels TITRATION CURVES and DNA concentrations, respectively (see Fig. 1c and Supplementary Figure 2c of the publication).

ROIs. The HiP-FA setup is very robust against small misalignments of the optical paths. However, after a new adjustment of the setup it is necessary to specify the two regions of interest (ROIs) corresponding on the raw data to the parallel and perpendicularly polarized components of the emitted fluorescence light (Supplementary Fig. 1b). In this example the parallel component is on top of the image and the perpendicular one on the bottom, but this could be readily inverted by switching “Flip data” to ON in the FILE panel. The two signals appear as Gaussian shaped patterns and the ROIs boundaries (in pixels) of two regions containing the Gaussian patterns can be defined the corresponding commands on the right hand side of the panel. Note that the choice of the ROIs does not need to be accurate since the HiP-FA method is insensitive to slight shifts of FA resulting from the choice of slightly different ROIs.

DNA CONCENTRATIONS. The accuracy of the method depends strongly of how well the DNA concentration $c(z,t)$ is determined by using the reference wells containing NB. The software first uses the calibration curve obtained from a direct titration of NB with a competitor DNA sequence (Supplementary Fig. 2a) to compute the competitor DNA concentration $c(z,t)$ for each reference well (thin colored lines in the figure of the panel; the averages of the individual curves are displayed as thick white points). The fitted parameter obtained by using the Hill Equation (V_{max} , k , n and y_0 ; see Supplementary Fig. 2a) have to be entered if the “Parameters Hill equation” part of the panel. Due to the relatively low affinity of NB to DNA ($\sim 2\mu M$), $c(z,t)$ can be determined accurately only for $c > \sim 100 nM$. The

concentrations below are extrapolated by fitting the averaged curve using a one-dimensional diffusion model (thick white line; see Methods). This fitting procedure for each z-slice (change “z” in panel SETTINGS for visualization) is critical for the proper construction of the titration curves. To optimize the fitting procedure, it is useful to apply different thresholds for the FA (“Tresh” in “Thresholds”), to fix the offset for the FA values of NB (“offset FA” as the minimum FA value for NB), or to limit the number of cycles to be considered for the fitting procedure (“Cycle End”). Some guess constants can be changed, but this is usually not necessary. Only the parameter “ t_0 ” need to be adjusted every time: this parameter corresponds to the time period (in cycles) between the production of the gel matrix and the actual beginning of the measurements (usually this should be < 10-20min in time). Once the quality of the fits are satisfying to each z-height, the DNA concentrations are defined even at low DNA concentrations and the titration curves can be analyzed.

TITRATION CURVES. One can visualize the individual titration curves using the “X (raw)” command of the SETTINGS panel. The fitting of the curved is achieved automatically online (in red) according to the procedure described in Methods. Two modes of fitting are possible: by default, all parameters are left free to evolve (see Methods). The concentration of the active protein (R_t) and the dissociation constant (K_{D2}) are displayed in red in the “Fitting parameters” part of the panel. For more robustness and given that usually the protein concentration is the same in every well, the concentration of the active protein can be fixed by switching the “Fix conc. R_{t0} ” to ON and its value can be set by using the command “ R_{t0} ”. The parameter B (see Methods) which corresponds to the lower offset of the titration curves is an additional free parameter that can be easily fixed and its value can be set by using the command “Offset”. The value usually corresponds to the FA of the unbound labelled reference DNA oligomer.

The results can be automatically exported by pressing the command “Export” of the TITRATION CURVES PANEL. The software creates a text file containing an ordered list of the fit parameters for all the measurement wells of the plate.

HiP-FA software / screenshot

